UCRL--87858

DE82 019103

CONF-8206102--2

UCRL-87858
PREPRINT

MICROFIELD DISTRIBUTION FOR DEGENERATE ELECTRONS

David B. Boercker
James W. Dufty

MASTER

This paper was prepared for presentation at
6th International Conference on Spectral Line
Shapes, Boulder, Colorado, July 12-16, 1982

July 1982

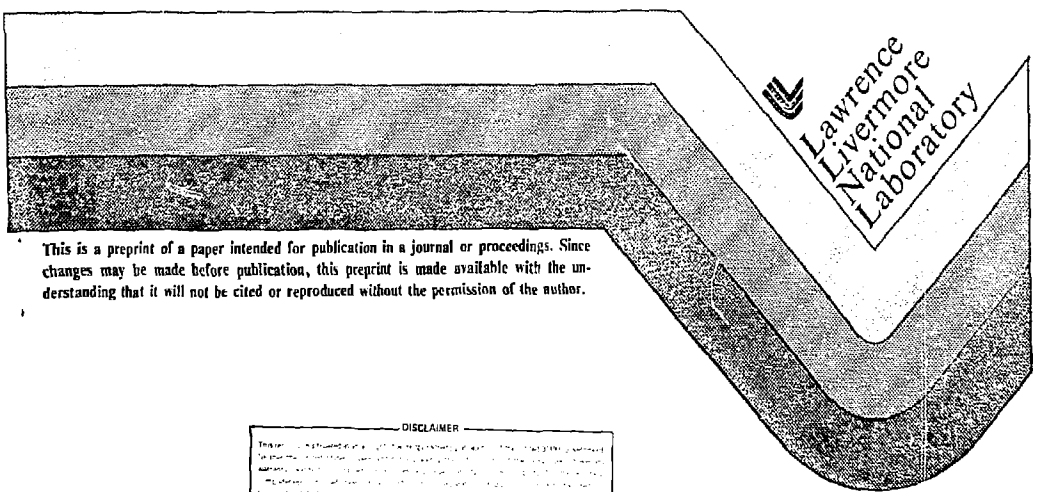

MICROFIELD DISTRIBUTION FOR DEGENERATE ELECTRONS

David B. Boercker

Lawrence Livermore Laboratory
University of California
Livermore CA 94450

James W. Dufty

Department of Physics
University of Florida
Gainesville FL 32611

Introduction

The description of spectral line shapes for atoms in a plasma incorporates the effects of both perturbing ions and perturbing electrons (1). Most theoretical formulations treat the ion effects as simple Stark splitting due to an ion field at the atom, with an average over the probability distribution for the values of such ion microfields. In contrast, the electron broadening is described through an electron-radiator collision operator. In this context, the calculation of ion electric microfield distribution has been of central importance (2), while the corresponding electron microfield distributions have been of less interest. However, a different approach has been developed that treats electrons and ions more symmetrically. This is the "model microfield method" (3), which requires the electron microfield distribution in addition to the ion microfield distribution. The structure of the theory is quite simple and has met with considerable success(4). The utility of the model microfield method is a primary motivation for the following consideration of the microfield distribution for electrons.

Both electrons and ions are well approximated by their classical limit, even for the relatively high densities observed in current laser-produced plasmas. However, it is expected that in the near future laser

compression will achieve even higher densities. The situation is illustrated in Figure 1 which shows several curves of constant fugacity, z, for an ideal Fermi gas in the temperature-density plane. The dots indicate the conditions achieved in typical laser expriments in recent years (5), while the box labelled LCP indicates the region which is generally considered to be accessible to the next generation of laser compressed plasmas. In addition, the box labelled LPS indicates the region being probed by laser produced shock experiments (6). Clearly, plasmas in this region and those in the upper left part of the LCP region require a full quantum mechanical treatment of the electrons. The prediction of spectral line shapes for these conditions using the model microfield method requires the microfield distributions for both ions and electrons. The objective here is to provide a quantum formulation of the electron distribution function, and analyze it for the simplest case of non-interacting electrons, the quantum Holtsmark distribution.

In the next section, the quantum microfield distribution is defined for the electron electric field distribution in a grand canonical ensemble. The definition is general, allowing for description of the distribution at a charged or neutral point and applies for the electron Coulomb field ("high frequency" microfield) or shielded field ("low frequency" microfield). By analogy with the Baranger-Mozer cluster expansion for the

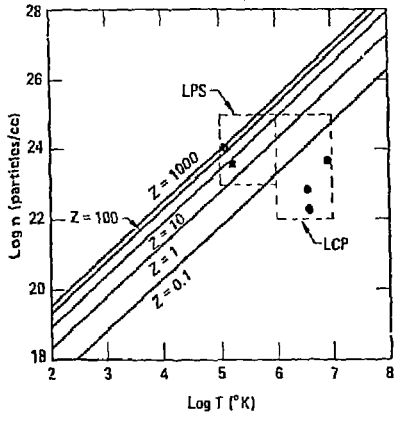

Figure 1 Contours of constant fugacity, z, for an ideal Fermi gas.

classical case (7) a cluster expansion for the microfield distribution is defined. The cluster series is resummed in section III to closed form for the case of no interactions, to define a quantum Holtsmark distribution. In this way the problem is reduced to a one-electron calculation. The usual classical result is verified in the limit of $z \ll 1$; the large and small field behavior is determined for arbitrary degeneracy.

Quantum Microfield Distribution

For classical systems, the Fourier transform of the electric microfield distribution can be written in terms of a series of cluster functions involving the correlations among progressively larger groups of particles (7). The purpose here is to demonstrate that the microfield distribution for a quantum system can be expressed in an identical manner with an appropriate generalization of the definition of the cluster functions.

In general, the microfield distribution is defined by

$$Q(\varepsilon) = \langle \delta(\vec{\varepsilon} - \vec{E}) \rangle \tag{1}$$

where $\vec{E}$ is the operator corresponding to the electric field (high or low frequency) and $\vec{\varepsilon}$ is one of its possible eigenvalues. The angular brackets indicate an equilibrium average over the grand canonical ensemble. It is convenient to use the Fourier representation of the delta function and to rewrite Eq. (1), as

$$Q(\varepsilon) = \int \frac{d\vec{\lambda}}{(2\pi)^3} e^{-i\vec{\varepsilon}\cdot\vec{\lambda}} F(\lambda) , \qquad F(\lambda) \equiv \langle e^{i\vec{\lambda}\cdot\vec{E}} \rangle \tag{2}$$

More explicitly, the grand canonical average in Eq. (2) is

$$F(\lambda) = \sum_{N \geq 0} \frac{z^N}{\Xi} \operatorname{Tr}_{1 \cdots N} e^{-\beta H_N} e^{i\vec{\lambda}\cdot\vec{E}_N} \tag{3}$$

where Ξ is the grand partition function, z is the fugacity and β is the inverse temperature. The Hamiltonian H_N and the electric field, $\vec{E}_N$, are

$$H_N \equiv \sum_{i=1}^{N} H(i) + \sum_{i<j}^{N} V(ij) \quad , \qquad \vec{E}_N \equiv \sum_{i=1}^{N} \vec{E}(i) \tag{4}$$

where $\vec{E}(i)$ is the contribution to the total field due to the i^{th} electron, V(ij) is the potential of interaction between the electrons, and H(i) is the single particle Hamiltonian. For a neutral point H(i) is the kinetic energy of the electron; for a charged point H(i) includes the electron-radiator potential as well. The trace in Eq. (3) is to be performed using anti-symmetrized states.

To proceed it is convenient to write

$$e^{i\vec{\lambda}\cdot\vec{E}_N} = \prod_{j=1}^{N} e^{i\vec{\lambda}\cdot\vec{E}(j)} = \prod_{j=1}^{N} (1 + \hat{\phi}(j)) \tag{5}$$

where, following Baranger and Mozer (7), the operator $\hat{\phi}$ is

$$\hat{\phi}(j) \equiv (e^{i\vec{\lambda}\cdot\vec{E}(j)} - 1) \tag{6}$$

Substituting Eq. (5) into Eq. (3) then yields

$$\begin{aligned} F(\lambda) &= \sum_{N>0} \frac{z^N}{\Xi} \operatorname{Tr}_{1\cdots N} e^{-\beta H_N} \prod_{i=1}^{N} (1 + \hat{\phi}(i)) \\ &= 1 + \sum_{s=1}^{\infty} \frac{1}{s!} \operatorname{Tr}_{1\cdots s} f^{(s)}(1\cdots s)\, \hat{\phi}(i)\cdots\hat{\phi}(s) \end{aligned} \tag{7}$$

The reduced distribution operators, $\hat{f}^{(s)}(1\cdots s)$, are defined by

$$\hat{f}^{(s)}(1\cdots s) = \sum_{N>s} \frac{z^N}{\Xi} \frac{N!}{(N-s)!} \operatorname{Tr}_{s+1\cdots N} e^{-\beta H_N} \tag{8}$$

or more explicitly, their position matrix elements are

$$\begin{aligned} f^{(s)}(r_1\cdots r_s; r'_1\cdots r'_s) = \sum_{N>s} \frac{z^N}{\Xi} \frac{N!}{(N-s)!} \int d^3\bar{r}_{s+1}\cdots d^3\bar{r}_N \\ \langle r_1\cdots r_s, \bar{r}_{s+1}\cdots\bar{r}_N | e^{-\beta H_N} | r'_1\cdots r'_s, \bar{r}_{s+1}\cdots\bar{r}_N \rangle \end{aligned} \tag{9}$$

where $|r\cdots r_N\rangle$ is an anti-symmetrized N-particle state. Because the $\hat{\phi}(i)$'s are diagonal in position representation, only the diagonal elements

in Eq. (9) are required in Eq. (7), and $F(\lambda)$ may be written as

$$F(\lambda) = 1 + \sum_{s=1}^{\infty} \frac{1}{s!} \int d^3r_1 \cdots d^3r_s \; f^{(s)}(r_1 \cdots r_s, r_1 \cdots r_s) \; \phi(r_1) \cdots \phi(r_s) \quad (10)$$

where $\phi(r)$ is the position matrix element of $\hat{\phi}$. The function $f^{(s)}(r_1 \cdots r_s; r_1 \cdots r_s)$ has the simple interpretation of being proportional to the probability that the s particles are located at the positions $\vec{r}_1 \cdots \vec{r}_s$. If the particles are uncorrelated this function factors into a product of single-particle functions and the sum in Eq. (10) may be performed immediately. When correlations due either to interactions or to exchange are present, $F(\lambda)$ may be written in a more appropriate form by introducing the correlation operators $h^{(s)}(r_1 \cdots r_s; r'_1 \cdots r'_s)$, through the definitions,

$$f^{(1)}(r_1; r'_1) = h^{(1)}(r_1; r'_1)$$

$$f^{(2)}(r_1, r_2; r'_1 r'_2) = h^{(2)}(r_1 r_2; r'_1 r'_2) + h^{(1)}(r_1; r'_1) \; h^{(1)}(r_2; r'_2) \quad (11)$$

etc. For $\ell \geq 2$, $h^{(\ell)}$ contains correlations due to both exchange and interactions. By introducing these functions into Eq. (10) and combining all those terms which vary only by the labelling of the integration variables, $F(\lambda)$ can be written in the desired form

$$F(\lambda) = 1 + \sum_{s=1}^{\infty} \frac{1}{s!} \sum_{\{m_\ell\}} \prod_{\ell} \frac{s!}{(\ell!)^{m_\ell} m_\ell!} (b_\ell)^{m_\ell}$$

$$= \exp\left\{\sum_{\ell=1}^{\infty} \frac{1}{\ell!} b_\ell\right\} \quad (12)$$

Here the sum over the m_ℓ's in the first line is restricted to those for which $\sum \ell m_\ell = s$, and the cluster functions b_ℓ are

$$b_\ell \equiv \int d^3r_1 \cdots d^3r_\ell \; h^{(\ell)}(r_1 \cdots r_\ell; r_1 \cdots r_\ell) \; \phi(r_1) \cdots \phi(r_\ell) \quad (13)$$

Equation (12) is the desired quantum mechanical generalization of the Baranger-Mozer expression for the Fourier transformed microfield. The utility of this formulation is that the correlation functions, $h^{(\ell)}$, vanish whenever one of the particles is sufficiently far away from the

remaining $\ell - 1$ particles. In the classical case "sufficiently far away" means outside the force range. In the quantum case, the correlation functions contain additional contributions that do not vanish until the particle is removed beyond a DeBroglie wave length from the others. For high temperatures this length is short and the exchange contributions to the correlation function can be ignored. For lower temperatures, the De Broglie wavelength can equal or exceed the average interparticle spacing and exchange effects become very important. The next section demonstrates how exchange modifies the Holtsmark distribution.

Quantum Holtsmark Distribution

In this section attention will be focused on the case of non-interacting particles. For the case of Fermi statistics the ideal gas contribution to $h^{(\ell)}(r_1 \cdots r_\ell ; r'_1 \cdots r'_\ell)$ is (8,9)

$$h_o^{(\ell)}(r_1 \cdots r_\ell ; r'_1 \cdots r'_\ell) = (-1)^{\ell-1} \sum_p h_o^{(1)}(r_1 ; r'_{p1}) h_o^{(1)}(r_2 ; r'_{p2}) \cdots h_o^{(1)}(r_\ell ; r'_{p\ell}) \tag{14}$$

Because of its cluster property, $h^{(\ell)}$ must correlate all ℓ particles, so the sum is restricted to the $(\ell-1)!$ possible cyclic permutations of ℓ objects. Using Eq. (14) in the expression for b_ℓ gives

$$b_\ell^{(0)} = (-1)^{\ell-1}(\ell-1)! \int d^3 r_1 \cdots d^3 r_\ell \, h_o^{(1)}(r_1 ; r_2)\phi(r_2) h_o^{(1)}(r_2 ; r_3)\phi(r_3) \cdots h_o^{(1)}(r_\ell ; r_1)\phi(r_1)$$

$$= (-1)^{\ell-1}(\ell-1)! \operatorname*{Tr}_1 (\hat{f}_o^{(1)} \hat{\phi})^\ell \tag{15}$$

Hence, $F(\lambda)$ becomes

$$F(\lambda) = \exp\left[\operatorname*{Tr}_1 \ln (1 + \hat{n}\hat{\phi})\right] \tag{16}$$

Here $\hat{n}$ is the ideal gas single particle distribution operator which gives the usual Fermi function when calculated in a representation which

diagonalizes H('). The above expression for $F(\lambda)$ is the main result of this section in that the quantum statistical mechanical average has been reduced to a definite single particle trace.

It is useful to indicate the non-degenerate ($z \ll 1$) limit of Eq. (16). In this case,

$$\hat{n} \to z e^{-\beta H(1)} \quad , \quad \ell n(1 + \hat{n}\phi) \to \hat{n}\phi,$$

so for a neutral point $F(\lambda)$ becomes

$$F(\lambda) = \exp\left[n \int d^3r \, (e^{i\vec{\lambda}\cdot\vec{E}} - 1)\right] \tag{17}$$

where $n = z/\lambda_T^3$ is the average density of a classical ideal gas. For the high frequency distribution, $\vec{E}$ is the Coulomb field and Eq. (17) may be written as

$$F(\lambda) = \exp\left(-e^{3/2} n\gamma\lambda^{3/2}\right) = \exp -(\lambda\varepsilon_o)^{3/2} \tag{18}$$

where $\gamma = \frac{4}{15}(2\pi)^{3/2}$ and $\varepsilon_o = e(\gamma n)^{2/3}$. Equation (18) is the usual Holtsmark result (10). The discussion in the subsequent sections will be limited to the high frequency distribution at a neutral point.

Large and Small Field Limits

As a consequence of the rotational invariance of the grand canonical average, the function, $F(\lambda)$, depends only on the magnitude of λ. Therefore, $Q(\varepsilon)$ in Eq. (2) may be written as

$$Q(\varepsilon) = \frac{1}{2\pi^2\varepsilon} \int_0^\infty d\lambda \; \lambda \sin(\lambda\varepsilon) F(\lambda) \tag{19}$$

It is usual to define the normalized distribution of field magnitudes by

$$P^*(b) \equiv \varepsilon_o 4\pi\varepsilon^2 Q(\varepsilon) = \frac{2b}{\pi} \int_0^\infty d\lambda \; \lambda \sin(\lambda b) F(\lambda/\varepsilon_o) \tag{20}$$

Here, $b \equiv \varepsilon/\varepsilon_0$, and ε_0 is the average field defined in Eq.(18). A change of variable $\lambda b \to \lambda$ gives the alternative expression,

$$P^*(b) = \frac{2}{\pi b} \int_0^\infty d\lambda \; \lambda \sin(\lambda) F(\lambda/b\varepsilon_0) \; . \tag{21}$$

It is evident in this form that the large b behavior of $P^*(b)$ is governed by the small λ dependence of $F(\lambda)$. Similarly, the behavior of $P^*(b)$ for small b has its dominant contribution from the large λ dependence of $F(\lambda)$. The dependence of $F(\lambda)$ on λ in these two limits is determined from Eq. (16) for arbitrary degeneracy in the appendix, and the results are used in this section to estimate the large and small field behavior of P^*.

1) Large field limit. As shown in the appendix, the small λ dependence of $F(\lambda/\varepsilon_0)$ is

$$F(\lambda/\varepsilon_0) \to \exp -\lambda^{3/2} \tag{22}$$

which is identical to the classical Holtsmark form Eq. (18). Consequently, the large field dependence of $P^*(b)$ is the same as that for the classical case, for all degrees of degeneracy. This is understandable from the fact that the asymptotically large field dependence is due to the field of a single nearest neighbor, and the presence of other electrons contributes only to deviations from the nearest neighbor asymptotic form. In the appendix, the first correction to the small λ dependence in Eq. (22) is also calculated, for strong degeneracy. The result is,

$$F(\lambda/\varepsilon_0) \to \exp -\left[\lambda^{3/2} + \frac{1}{2}\lambda^3\right] \tag{23}$$

Substitution into Eq.(21) gives for the large b dependence of $P^*(b)$,

$$P^*(b) \to \frac{1.5}{b^{5/2}}\left[1 + \frac{\nu}{b^{3/2}} + \cdots\right] \tag{24}$$

As indicated above, the leading term proportional to $b^{-5/2}$ is the same at all degrees of degeneracy. The first correction term is given by $\nu \sim 5.1$ in the classical limit. However, the strong degeneracy result from (23)

is $\nu=0$. This means that the effect of degeneracy is to decrease the probability for large fields, relative to the classical result.

2) Small field limit. The asymptotic behavior of $F(\lambda/\varepsilon_o)$ for large λ is given by Eq.(A.15) of the appendix,

$$F(\lambda/\varepsilon_o) \to \exp -[c(z)\lambda]^{3/2} \tag{25}$$

where $c(z)$ is given by Eq.(A.16). Use of (25) in Eq.(20) then provides the small field expansion of $P^*(b)$,

$$P^*(b) \to .424\ c^{-1} \left(\frac{b}{c}\right)^2 \left[1 - .463 \left(\frac{b}{c}\right)^2\right] \tag{26}$$

The function $c(z)$ goes to 1 for small z (non-degenerate limit) and Eq.(26) becomes the small field expansion of the classical Holtsmark distribution. For large z (strong degeneracy) $c(z)$ goes to zero as $z^{-2/3}$ (see Table 1 in the appendix for typical values). This means that the effect of degeneracy for small fields is to increase their probability relative to the classical result.

The above analysis of the large and small field limits suggests the following general behavior of the quantum Holtsmark function. As the degeneracy increases, the probability for larger fields decreases. Due to normalization the probability must therefore increase elsewhere, and this is seen to occur in particular for very small fields. For very strong degeneracy the probability density for fields near zero grows as z^2 so that the maximum of the distribution shifts toward the origin. The $b^{-5/2}$ tail remains for large fields however, since it is a single electron contribution and is unaffected by degeneracy effects.

To illustrate this behavior, it is useful to note that the low field result, Eq. (25), implies the relationship

$$P^*(b) \to c^{-1}\ P_o^*(b/c), \tag{27}$$

for small b, where $P_0^*(b)$ is the classical Holtsmark distribution. Figure 2 illustrates $P^*(b)$ from Eq.(27) in the small field region for several values of z (the dashed curve is the classical Holtsmark function, corresponding to c=1). Equation (27) is only valid asymptotically for small b so it is not implied that the curves in Figure 2 are accurate over the entire range shown. However, they do illustrate qualitatively the effect of degeneracy to increase the microfield distribution for smaller field values. Similarly the decrease in the distribution for large fields is shown in Figure 3, where $P^*(b)$ from Eq.(24) has been plotted for the classical case (v=5.1) and the strongly degenerate case (v=0).

Discussion

The analysis of section II suggests how the effect of interactions also could be accounted for. If $F_0(\lambda)$ denotes the quantum ideal gas contribution to $F(\lambda)$, i.e. that given in section III, then $F(\lambda)$ may be written as

$$F(\lambda) = F_0(\lambda) \exp\Big[\sum_{\ell=2}^{\infty} \frac{1}{\ell!} \left(b_\ell - b_\ell^{(0)}\right)\Big] \tag{28}$$

where b_ℓ and $b_\ell^{(0)}$ are defined by Eqs. (13) and (15), respectively. The difference $b_\ell - b_\ell^{(0)}$ is now non-zero due to electron-electron interactions. Retaining only the ℓ=2 term (as in the classical approximation of Baranger and Mozer) leads to

$$F(\lambda) = F_0(\lambda) \exp\Big[\frac{1}{2} \int d\vec{r}_1 d\vec{r}_2 \; g_2(r_1,r_2)\phi(r_1)\phi(r_2)\Big] \tag{29}$$

with

$$g_2(r_1,r_2) \equiv f^{(2)}(r_1,r_2;r_1,r_2) - f^{(1)}(r_1;r_1)f^{(1)}(r_2;r_2)$$

$$+ f^{(1)}(r_1;r_2)f^{(1)}(r_2;r_1) \tag{30}$$

The result (29) is formally identical to that of Mozer and Baranger (7). Furthermore, the expression for $g_2(r_1,r_2)$ reduces in the classical limit to the corresponding quantity defined by them. They make the further approximation of evaluating g_2 in the Debye-Huckel approximation. The

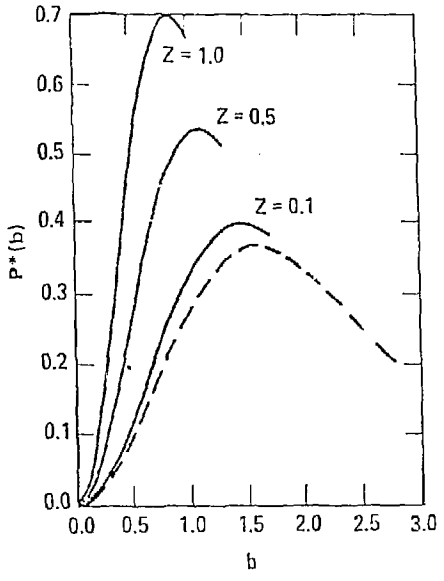

Figure 2 The small-field form of $P^*(b)$, (Eq. (27)) for several values of z the dashed curve is the classical Holtsmark function, z=0.

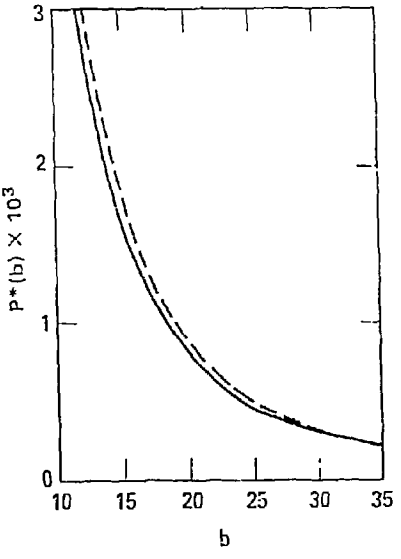

Figure 3 The large-field form of $P^*(b)$, (Eq. (24)); —— quantum, - - - classical.

quantum generalization of this approximation is the random phase approximation, valid for all degeneracies and incorporating Debye-Huckel as the classical limit.

Acknowledgment

The authors are indebted to C.F. Hooper for his support and encouragement. The work of DBB was performed under the auspicies of the U.S. Department of Energy by Lawrence Livermore Laboratory under contract #W-7405-Eng-48; JWD was supported by the Department of Energy and the National Science Foundation.

References

1. Griem, H.R.: Spectral Line Broadening by Plasmas, (Academic Press, N.Y., 1974).
2. Hooper, C.F.: Phys. Rev. 165, 215 (1968).
3. Brissand, A., Frisch, U.: JQSRT 11, 1761 (1971); Dufty, J.W.: in Spectral Line Shapes, B. Wende, editor (de Gruyter, Berlin, 1981).
4. Seidel, J.: Z. Naturforsch, 32a, 1207 (1977), and in Spectral Line Shapes, (ibid).
5. See, for example, Haur, A., in Spectral Line Shapes, (ibid), and references therein.
6. Trainor, R.J., Shaner, J.W., Auerbach, J.M., Holmes, N.C.: Phys. Rev. Lett. 42, 1154 (1979).
7. Baranger, M., Mozer, B.: Phys. Rev. 115, 521 (1959); 118, 626 (1960).
8. Isihara, A.: Statistical Physics, (Academic Press, NY, 1971).
9. Munster, A.: Statistical Thermodynamics, Vol. 1, Chapter 9 (Springer-Verlag, Berlin, 1969).
10. Holtsmark, J.: Ann. Physik 58, 577 (1919); Chandresekhar, S.: Rev. Mod. Phys. 15, 1 (1943).

Appendix - Asymptotic Forms of $F(\lambda)$

In this appendix the expression for $F(\lambda)$ given by Eq. (16) is evaluated to determine the asymptotic behavior for large and small λ. It is convenient to represent Eq. (16) in the following form,

$$F(\lambda) = \exp \int_0^1 dx \operatorname{Tr}_1 \hat{M}(x)\hat{n} , \quad \hat{M}(x) \equiv \hat{\phi} (1 + x\hat{n}\hat{\phi})^{-1} \tag{A.1}$$

Evaluating the trace in momentum representation gives

$$F(\lambda) = \exp \int_0^1 dx \int \frac{d\vec{p}}{h^3} M(p,p)n(p) \tag{A.2}$$

where, from Eq. (A.1) $M(p,p')$ is the solution to the integral equation,

$$M(p,p') = \tilde{\phi}(\vec{p}-\vec{p}') - x \int d\vec{p}'' M(p,p'')n(p'')\tilde{\phi}(\vec{p}''-\vec{p}') \tag{A.3}$$

Also, $n(p)$ is the Fermi function and $\tilde{\phi}(p)$ is the Fourier transform of $\phi(r)$,

$$\tilde{\phi}(\vec{p}) = \int d\vec{r}\, e^{i\vec{p}\cdot\vec{r}/\hbar} \left[e^{i\vec{\lambda}e\cdot\hat{r}/r^2} - 1\right] \tag{A.4}$$

Here $\hat{r}$ is the unit vector associated $\vec{r}$, respectively.

Consider first the behavior of $F(\lambda)$ for small λ. It is appropriate to introduce the dimensionless variables $\vec{p}' = \vec{p}/p_0$, $\vec{r}' = \vec{r}/(e\lambda)^{1/2}$, and $\lambda' = \lambda\varepsilon_0$, where p_0 is a measure of the average electron momentum. Using these variables in Eq. (A.2) and Eq. (A.3) and deleting the primes yields

$$F(\lambda/\varepsilon_0) = \exp \int_0^1 dx \int \frac{d\vec{p}}{(2\pi)^3} M^*(p,p)n^*(p) \tag{A.5}$$

with

$$n^*(p) \equiv \left(z^{-1} e^{ap^2} + 1\right)^{-1}$$

$$M^*(p,p') = \phi^*(\vec{p}-\vec{p}') - x \int \frac{d\vec{p}''}{(2\pi)^3} M^*(p,p'')n^*(p'')\phi^*(\vec{p}''-\vec{p}')$$

$$\phi^*(\vec{p}) = (\lambda\sigma^2)^{3/2} \int d\vec{r}\, e^{i\sqrt{\lambda}\,\sigma\,\vec{p}\cdot\vec{r}} \left[e^{i\hat{\lambda}\cdot\hat{r}/r^2} - 1\right] \tag{A.6}$$

Here $\sigma \equiv (ep_0^2/\hbar^2\varepsilon_0)^{1/2}$ and $a \equiv p_0^2/2mk_BT$. It follows immediately that for small $\lambda\sigma^2$, $\phi^*(\vec{p})$ approaches

$$\phi^*(p) \to \phi^*(o) = (\lambda\sigma^2)^{3/2} \int d\vec{r} \left[e^{i\hat{\lambda}\cdot\hat{r}/r^2} - 1\right] \tag{A.7}$$

and the leading contributions to $M^*(p,p')$ are

$$M^*(p,p') \to \phi^*(o) - x \int d\vec{p}'' \phi^*(o) n^*(p'') \phi^*(o) \tag{A.8}$$

Use of this result in (A.5) gives the desired small λ behavior for $F(\lambda/\varepsilon_o)$

$$F(\lambda/\varepsilon_o) \to \exp - \left[\lambda^{3/2} + \frac{1}{2}\lambda^3\right] . \tag{A.9}$$

Some qualification of this result is necessary. The leading term in (A.9) is due to the first term on the right side of Eq. (A.8). The zero argument in this term does not require the limit taken in Eq. (A.7) because only the contribution from the diagonal part of $M(p,p')$ is required for $F(\lambda)$. In contrast, the first correction term of order λ^3 in Eq. (A.9) does come from application of the limit taken in Eq. (A.7). This limit is not uniform with respect to the degree of degeneracy because of the combination $\lambda\sigma^2$. For strong degeneracy, $p_o \sim \hbar n^{1/3}$, so $\sigma \sim 1$ and the limiting form of (A.7) is an accurate representation. However, for small degeneracy $p_o \sim \sqrt{2mk_BT}$, so σ is large and Eq. (A.7) does not give the small λ limit. Consequently the leading $\lambda^{3/2}$ term in (A.9) is exact for all degeneracies, but the correction term proportional to λ^3 is valid only for strong degeneracy.

Next consider the dependence of $F(\lambda/\varepsilon_o)$ for large λ. Make the change of variables $\sqrt{\lambda}\ \sigma\ \vec{p} \to \vec{p}$ in Eqs. (A.5) and (A.6) to give,

$$F(\lambda/\varepsilon_o) = \exp \int_0^1 dx \int \frac{d\vec{p}}{(2\pi)^3} \bar{M}(p,p) n^*(p/\sqrt{\lambda}\ \sigma) \tag{A.10}$$

and $\bar{M}(p,p') \equiv (\lambda\sigma^2)^{-3/2} M^*(p/\sqrt{\lambda}\ \sigma,\ p'/\sqrt{\lambda}\ \sigma)$ obeys the equation

$$\bar{M}(p,p') = \bar{\phi}(\vec{p}-\vec{p}') - x \int \frac{d\vec{p}''}{(2\pi)^3} \bar{M}(p,p'')n^*(p''/\sqrt{\lambda}\,\sigma)\bar{\phi}(\vec{p}''-\vec{p}') \quad (A.11)$$

with

$$\bar{\phi}(\vec{p}) \equiv \int d\vec{r}\; e^{i\vec{p}\cdot\vec{r}} \left[e^{i\hat{\lambda}\cdot\hat{r}/r^2} - 1\right] . \quad (A.12)$$

For large $\lambda\sigma^2$, $n^*(p/\sqrt{\lambda}\,\sigma) \to \alpha(z) \equiv z/(1+z)$, and the equation for $\bar{M}(p,p')$ becomes

$$\bar{M}(p,p') = \bar{\phi}(\vec{p}-\vec{p}') - x\alpha \int \frac{d\vec{p}''}{(2\pi)^3} \bar{M}(p,p'')\bar{\phi}(\vec{p}''-\vec{p}') \quad (A.13)$$

It follows that $\bar{M}(p,p') = \bar{M}(\vec{p}-\vec{p}')$ and Eq.(A.15) can be solved by Fourier transformation,

$$\bar{M}(\vec{p},\vec{p}') = \int d\vec{r}\; e^{i(\vec{p}-\vec{p}')\cdot\vec{r}} \frac{\phi(r)}{1 + x\alpha\phi(r)} \quad (A.14)$$

Substitution of Eq. (A.14) into (A.9) then gives the large λ behavior for $F(\lambda/\varepsilon_0)$,

$$F(\lambda/\varepsilon_0) \to \exp -\left[c(z)\lambda\right]^{3/2} \quad (A.15)$$

with

$$\left[c(z)\right]^{3/2} \equiv -\frac{1}{\gamma_\alpha} \int d\vec{r}\; \ln\left[1 + \alpha\left(e^{i\hat{\lambda}\cdot\hat{r}/r^2} - 1\right)\right] \quad (A.16)$$

The values of c(z) for several values of z are shown in Table 1.

Table 1. c(z) for typical values of z

z	c(z)	z	c(z)
0.0	1.00	0.8	.578
0.1	.914	1.0	.525
0.2	.843	2.0	.431
0.4	.730	5.0	.288
0.6	.644	10.0	.197